Aquaporins and water control in drought-stressed poplar leaves: A glimpse into the extraxylem vascular territories

Beatriz Muries Bosch, Robin Mom, Pierrick Benoit, Nicole Brunel-Michac, Hervé Cochard, Patricia Roeckel-Drevet, Gilles Petel, Eric Badel, Boris Fumanal, Aurelie Gousset, et al.

MURIES Beatriz[a], MOM Robin[a], BENOIT Pierrick[a], BRUNEL-MICHAC Nicole[a], COCHARD Hervé[a], DREVET Patricia[a], PETEL Gilles[a], BADEL Eric[a], FUMANAL Boris[a], GOUSSET-DUPONT Aurélie[a], JULIEN Jean-Louis[a], LABEL Philippe[a], AUGUIN Daniel[b], VENISSE Jean-Stéphane[a]*

Aquaporins and water control in drought-stressed poplar leaves: a glimpse into the extraxylem vascular territories

AUTHORS' E-MAIL ADDRESSES:

bmuries@gmail.com

robin.mom@etu.uca.fr

pierrickfrom@free.fr

nicole.brunel@uca.fr

herve.cochard@inra.fr

patricia.drevet@uca.fr

gilles.petel@uca.fr

eric.badel@inra.fr

boris.fumanal@uca.fr

aurelie.gousset@uca.fr

Jean-Louis.JULIEN@uca.fr

philippe.label@uca.fr

auguin@univ-orleans.fr

j-stephane.venisse@uca.fr

Abstract

Leaf hydraulic conductance (K_{leaf}) and capacitance (C_{leaf}) are among the key parameters in plant-water regulation. Understanding the responses of these hydraulic traits to drought conditions remains a challenge for describing comprehensive plant-water relationships. The ability of an organism to resist and/or tolerate embolism events, which may occur at high negative pressure caused by hydric stress, relies on how well it can sustain a hydraulic system in a dynamic equilibrium. *Populus deltoides* is a water-saving tree species with a stomatal conductance that declines rapidly with reduced water availability. Under unfavorable conditions, the stomatal control of transpiration is known to be closely coordinated with a loss of plant hydraulic functioning that can ultimately result in hydraulic failure through xylem embolism, notably in leaves. The effects of drought on leaf hydraulics are also related to regulation in water permeases such as the aquaporins. To describe the responses linked to leaf hydraulics under severe drought and rewatering conditions, water-stressed poplars were monitored daily on an ecophysiological and a molecular scale. A structural and expression analysis on a set of aquaporins was carried out in parallel by *in situ* hybridization analysis and quantitative PCR. In complement, water distribution in water-challenged leaves was investigated using X-ray microtomography. A general depression of leaf hydraulic conductance and relative water content occurred under drought, but was reversed when plants were rewatered. More interestingly, (i) extreme leaf water deficiency led to marked xylem and lamina embolism, but a degree of hydric integrity in the midrib extraxylem territories and the bundle sheath of the minor veins was maintained, and (ii) the sub-tissue water allocation correlated well with an over-accumulation of several *PIP* and *TIP* aquaporins. Our multi-facet molecular ecophysiological approach revealed that leaves were able to secure a certain level of hydric status, in particular in cell territories near the “living ribs”, which provided rapid hydric adjustment responses once favorable conditions were restored. These findings contribute to an integrated approach to leaf hydraulics, thus favoring a better understanding of the cell mechanisms involved in tree vulnerability to climate changes.

KEY WORDS

Populus, Leaf, Extraxylem territories, Bundle sheath cells, Aquaporins, Cavitation

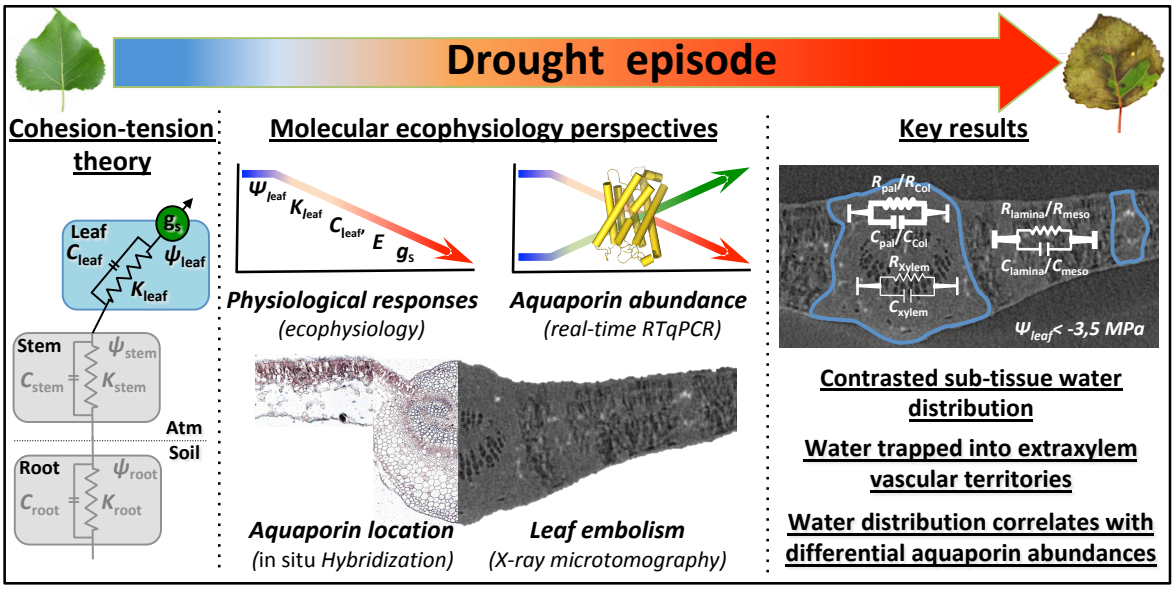

66

67 **Highlights**

68 Poplar, an important woody crop is sensitive to water availability.

69 Soil water supply substantially affects various ecophysiological traits linked to plant hydraulic
70 status and aquaporin abundance.

71 When xylem is embolized, extraxylem vascular territories and minor veins stay fully hydrated
72 and can be considered as “capacitors”.

73 These capacitors would act as water pools in the leaves, pivotal lever to drought tolerance
74 and recovery.

75 Specific sub-tissue water allocation correlates with differential PIP and TIP aquaporin
76 abundances.

1. Introduction

Water movement throughout a plant depends not only on stomatal aperture, but also on the interconnected dynamic hydraulic conductances from roots, stem and leaves (Sack and Holbrook, 2006; Heinen et al., 2009). Water potential gradient caused by plant transpiration is the main driving force of these water transfers. In the cohesion-tension theory, transpiration into the atmosphere draws water from the soil along a root-stem-leaf continuum, creating a gradient in water potential (Ψ_w). Tension in the vascular system can reach very high levels, generating a thermodynamically highly metastable biophysical state. During drought, low soil water content exacerbates this tension. As a result, the sap tensions can exceed a threshold value above which vaporization can occur in the xylem conduit and disrupt water columns in the lumen of xylem vessels, an effect called cavitation. The resulting embolized conduits become non-functional for water supply. This process is widely believed to be a substantial cause of the decline in plant hydraulic conductance that occurs during drought. It can ultimately precipitate premature mortality of plant organs (including leaves), and sometimes plant death (Choat et al., 2012). A very extensive and intricate pattern of veins adorns leaves. Embolism events are theoretically expected to propagate between interconnected conduits, suggesting that the leaf could be an organ highly vulnerable to dehydration. However, *in vivo*, the network architecture plays a substantial role in the differential propagation of embolism. Interestingly, a high gradient in vulnerabilities to dehydration is observed and depends on the hierarchic level of venation: embolism vulnerability increases proportionally with the size of veins, and the initial nucleation occurs in the largest veins (Scoffoni and Jansen, 2016, Brodribb et al., 2016ab; Hochberg et al., 2107; Scoffoni et al., 2017ab-2018). As leaves form a major hydraulic bottleneck impacting overall plant hydraulic responses (Sack and Holbrook, 2006), deciphering the mechanisms of embolism and their effects on hydraulic function in leaves is an essential adjunct to studies on stems.

By its position within the canopy, the leaf system experiences widely fluctuating ambient conditions such as irradiance and temperature, while depending on the hydric status of the tree overall (Dobra et al., 2010). Most environmental stresses share common effects and adaptive responses in leaf physiology, but they usually result in hydraulic disruptions, cavitation in veins, and tissue dehydration in leaves. Dehydration status arises from an imbalance between tissue water uptake or storage, and tissue reallocation or loss through transpiration (Jackson et al., 2003). As an adaptive response, leaves rapidly close their stomata to modulate stomatal conductance (g_s). However, transpiration is involved in carbon uptake for photosynthesis and general metabolism, and in preventing heat damage in leaves exposed to full sunlight. But for plant species that exhibit high sensitivities to drought stress,

impaired transpiration thus becomes hazardous in leaf tissues. Concomitantly, osmotic adjustments can occur, involving the neo-synthesis and/or accumulation of small compatible solutes (or osmolytes), *e.g*. proline, sugars, glycine betaine and some inorganic ions (Khan et al., 2010). These entities help the cells maintain the structural integrity of membranes and intrinsic molecular components that are in a dehydrated state. A barely explored hypothesis is that dehydrated leaf tissues or cells can buffer variations in leaf water potentials by using their own water storage: plant tissues can safeguard cell integrity (*i.e.* metabolism) by buffering the effects of small fluctuations in water potential. By analogy with an electric circuit (van den Honert, 1948), this property is termed hydric capacitance (Koide et al., 1989).

Physiologically, leaf water storage capacitance C_{leaf} measures the ability of a leaf to store and reallocate water to buffer its own hydraulic status. Relative intrinsic capacitance is defined as the mass of water that can be extracted, *i.e.* reallocated, per unit change in the water potential of the tissue. By definition, capacitance fundamentally integrates the complex water network of a tissue, working in parallel with the water transport efficiency (hydraulic conductance, K_h) and in series with the absolute water storage capacity (or relative water content, RWC) of the tissue. Despite its importance, leaf capacitance has been paradoxically under-investigated.

The relevance of C_{leaf} is clearly evidenced in desert succulent plants, which are highly persistent in water-limited environments. Interestingly, these species present a water transport from the water-storing parenchyma to the photosynthesizing collenchyma (*a.k.a.* "*chlorenchyma*"), displaying contrasting capacitance between these two distinct but neighboring cell types: high *C* for water storage parenchyma cells and lower *C* for chlorenchyma (Schmidt and Kaiser, 1987; Smith et al., 1987; Tissue et al., 1991; Vendramini et al., 2002; Nobel, 2006). A high-capacitance water-storing parenchyma with stable water potential gradients is thought to provide an efficient mechanism to ensure a supply of water from its storage tissues that actively sustains photosynthesizing cells for longer in periods of drought (Martin et al., 2004; Nobel, 2006). In temperate woody species without prominent leaf water storage tissues, osmotic and hydrostatic pressures affect inter-tissue water transfer and related capacitances. Even though C_{leaf} is a well-defined parameter, it is still neglected when assessing the vulnerability of leaves to drought-induced hydraulic dysfunction, "leaf water storage" being the preferred concept. Overall, it is assumed that leaves with high K_{leaf} values and high maximum transpiration levels benefit most from stored water to buffer fluctuations of available water (Aasamaa and Sober, 2001; Aasamaa et al., 2001; Sack et al., 2003). There is a need for a better understanding of this hydraulic trait, C_{leaf}, and especially of the underlying molecular mechanisms that govern it.

Leaves, and especially their veins, function as microfluidic circuitry. The hydraulic resistances are not constant, but dynamic, and can vary nonlinearly with water potential. In addition, this ecophysiological trait primarily concerns a living structure, the cell, which is delimited by a semi-permeable membrane. Thus these dynamic water movements across biological membranes are fundamental for maintaining proper fluid balance within and between cells, and within different anatomic compartments (inner leaf tissues such as xylem parenchyma, bundle sheaths and mesophyll cells). Models of dynamic hydraulic flow in tissues and organs integrate aquaporins (AQP) as molecular actors in the regulation mechanism (Sade and Moshelion, 2016).

AQP are membrane-spanning proteins that were assigned to the superfamily of the major intrinsic proteins (MIP). They are involved in the specific transport of water and small neutral solutes or dissolved gases across plasma and intracellular membranes (Prado and Maurel, 2013; Chaumont and Tyerman, 2014). These selective channels are present in all life forms, whether mammals, amphibia, insects, plants, or bacteria (Heymann and Engel, 1999). In angiosperms, several subfamilies of MIPs have been identified, typically clustered into five main subfamilies with the plasma membrane intrinsic proteins (PIP), tonoplast intrinsic proteins (TIP), nodulin-like intrinsic proteins (NIP), small basic intrinsic proteins (SIP) and the non-exclusive *X*-intrinsic proteins (XIP) (Danielson and Johanson, 2008; Anderberg et al., 2012). Plant AQPs show a remarkable diversity: *Populus* exhibits 54 AQP members from all five subclasses (Gupta and Sankararamakrishnan, 2009; Lopez et al., 2012). Some of them have been extensively investigated, and recent insights into their structural signatures, expression patterns, subcellular localizations, and substrate specificities have led to models that target the regulation of transport activity in various physiological plant processes. Yet despite extensive research into aquaporin function and regulation for coordinated dynamics of K_{leaf} or g_s (Heckwolf et al., 2011; Ben Baaziz et al., 2012; Ferrio et al., 2012; Lopez et al., 2013), studies of their potential physiological roles in regulating leaf capacitance in plants challenged by unfavorable drought conditions are still sparse (Vitali et al., 2016).

In this study, we designed an experiment in which a set of poplar trees experienced a gradual controlled drought for several days, followed by rehydration. Based on leaf ecophysiological response, we monitored the molecular response, focusing on the contributions of PIP and TIP aquaporin subfamilies by analyzing the accumulation transcript patterns of all related members and the spatial distribution of some of those most expressed. We also investigated where the embolism events occurred in leaf veins during leaf dehydration to turgor loss and beyond, using X-ray microtomography (microCT), which allows direct visualization of embolized conduits and their anatomic characteristics in

different vein orders. We discuss our results in terms of ecophysiological, molecular and structural findings.

2. Materials and Methods

2.1. Plant material and drought experimental design

Experiments were conducted on two-year-old *Populus* trees (*Populus deltoides*, Marsh) cultivated in 20 liter pots filled with commercial substrate (40% black, 30% brown and 30% blond peat moss, pH 6.1, DUMONA-RN 75-3851, Arandon, the Netherlands). Plants were grown in a controlled-environment greenhouse (Clermont Auvergne University, Clermont-Ferrand, France) under a 16 h light/8 h dark photoperiod at 18-22°C (night / day) and with relative humidity set at 70±10%. When incoming sunlight in the greenhouse was below 350 µmol m^{-2} s^{-1} (dawn and dusk), photosynthetic photon flux was maintained using 400W Master son-T Pia Hg-free lamps (Philips). Three weeks beforehand, and during the experiments, the plants were placed in an open but controlled environment where day/night temperatures were around 17°C and 26°C, respectively, and the PAR at midday were around 1450 µmol m^{-2} s^{-1}; conditions are detailed in Supplemental Figures S1. Pots were automatically watered by drip irrigation, maintaining daily field capacity. For the experiment, three control plants were continuously well-watered (number of trees sufficient for a control physiological situation because of the very homogeneous responsiveness of *Populus deltoides*), and nine plants were drought-challenged by withholding irrigation (greater number of trees to cover eventual heterogeneous responsiveness during stressful conditions). Once the hydric stress was reached (Ψ_{leaf} < -3,5 MPa), but before the earliest signs of leaf wilting (for Ψ_{leaf} between -3,5 MPa and -4 MPa for *Populus deltoides* in our environmental conditions), droughted plants were rewatered. During the rehydration phase, four kinetic points were targeted: 12 h after rewatering (Day 9 of experimentation), two days after rewatering (Day 10 of experimentation, which corresponded to no significant change in ecophysiological traits), three days after rewatering (Day 11 of experimentation, which corresponded to a significant early transpiration recovery) and ten days after rewatering (Day 18 of experimentation when the predawn Ψ_{leaf} = 0.0 MPa, and when the transpiration rate was fully recovered). The water stress conditions of seven plants (three control and four stressed plants) were indirectly assessed through water loss by evapotranspiration by measuring the micro-variations in stem diameters and the total mass of the experimental system (Figure 1). The micro-variations in stem diameters were continuously measured using linear variable displacement transducers (LVDTs) (LVDT model DF5, Solartron Metrology, Massy, France) connected to a data acquisition system (CR3000 Micrologger, Campbell Scientific, Inc., Logan, UT, USA). LVDTs were installed at a height of 10 cm from the base of the trunk. Changes in diameter variation (accuracy < 1 µm) were logged at 10 s intervals, and 5 min means were recorded. Experimental systems (*i.e.* pot and plant) were continuously weighed to check water deficit by placing them on a calibrated scale (PCE-

BDM-15, readability from 0.1 g, PCE, France) connected to a data acquisition system (CR1000, Campbell Scientific). For the ecophysiological and molecular analysis, fully expanded leaves from the top of each tree were sampled.

2.2. Leaf water potentials and gas exchange parameters

Predawn (5:00) and midday (14:00) leaf water potentials (Ψ_{leaf}) were measured using a Scholander pressure chamber (PMS Instrument Company, Model 1505 D, Albany, OR, USA). Daily predawn and midday leaf stomatal conductance (g_s) and transpiration flux (E) were measured with a portable photosynthesis measurement system (LI-1600, Li-Cor, Lincoln, NE, USA) under ambient conditions. Leaf hydraulic conductance (K_{leaf}) was assessed according to Attia et al. (2015), and calculated by using the equation K_{leaf} = E / (Ψ_{stem}-Ψ_{leaf}). This approach uses the ratio of the transpiration flux (E) to the water potential difference ($\Delta\Psi$) between the xylem at the leaf entry (Ψ_{stem}) and the bulk leaf (Ψ_{leaf}). E measurements were made with the LI-COR portable photosynthesis system (Li-1600), and Ψ_{leaf} was monitored immediately after with the Scholander pressure chamber. Predawn K_{leaf} calculation (at 05:00) was enabled by non-zero predawn E values. Stem xylem water potential (Ψ_{stem}) was estimated at 05:00am and 2:00pm by sealing three leaves for each analysis in a plastic bag wrapped in aluminum foil in the late afternoon of the day before measurement. Each Ψ_{stem} corresponds to the mean of the water potentials monitored from these three leaves. Transpiration was thereby prevented, and water tension was promoted to equilibrium at the point of attachment of the leaf to the stem (Begg and Turner, 1970). Leaf area (m^2) was measured using an ImageJ macro after scanning. A Höfler diagram determination is based on the pressure-volume curve theory according to Tyree and Hammel (1972). To construct the Höfler diagram and plot the related PV curve, changes in water potential and relative water content θ (%)=[(FW - DW) / (TW - DW) x 100] were monitored as the tissue dehydrated (where FW, DW, and TW are the fresh, dry and turgid masses, respectively). This relationship was quantified by allowing excised tissues (such as defoliated leaves) to slowly and artificially desiccate on a laboratory bench during which time water potentials and tissue weight were periodically measured. Leaf water storage capacitance per unit leaf area and unit water content (C_{leaf}; $\Delta\theta / \Delta\Psi.s^{-1}$) was obtained from these PV curves according to the procedures of Sack et al. (2003), Sack and Pasquet-Kok (2011) and Scholz et al. (2010).

2.3. Quantitative reverse transcription polymerase chain reaction analysis (RT- q*PCR)*

One leaf from three trees (which corresponds to three independent biological replicates) was sampled at 5:00am and 2:00pm, at Days -1, 6, 7, 8, 9, 10, 11 and 18 of the experimentation. Sampled leaves were depetiolated and immediately frozen in liquid nitrogen for subsequent molecular analysis. For total RNA extraction, samples (25-100 mg) were ground to a fine

powder in liquid nitrogen and stored at -80°C until use. Total RNA was extracted according to Chang et al. (1993) with some modifications. Briefly, leaf powders were transferred into 1 ml of lysis CTAB extraction buffer (cetyltrimethylammonium bromide). The homogenate was incubated for 5 min at 65°C and treated twice with 1 volume of chloroform:isoamyl alcohol (24:1). The supernatant was collected and treated overnight in 2 M LiCl at -20°C. The precipitate was collected by centrifugation (16,000 *g* for 45 min) and was washed with 70% ethanol. The pellet was dissolved in 25 µl of water (DEPC), and treated with 10 U RNAse-free DNAse (Promega, Madison, WI, U.S.A.) for 30 min. After two chloroform:isoamyl alcohol (24:1) washes, total RNA was precipitated with 100% ethanol (2V) 2 h at -20°C. After centrifugation at 16,000 *g* for 30 min, the pellet was washed with 70% ethanol, dissolved in 50 µl of water (DEPC) and stored at -80°C for further analysis. RNA concentrations were determined by spectrophotometry (OD 260/280) (spectrophotometer ND-1000, Nanodrop, France), and quality was checked using 2% TAE/agarose electrophoresis. First-strand cDNA was synthesized from 2 µg of total RNA using the SuperScript® III First-Strand Synthesis System for RT-PCR (Invitrogen™) and with oligo-dT, following the manufacturer's instructions. The synthesized cDNA was diluted 10-fold with sterile water and used as a template for PCR. The abundance of defense-related transcripts was determined by real-time Q-PCR with an MyiQ instrument (Bio-Rad), using the comparative C_t method. PCR was performed in a 96-well plate with a total volume of 15 µl, containing 10 µl of MESA GREEN qPCR MasterMix Plus (Eurogentec), 0.5 µM (each) of forward and reverse primers, and 2 µl of cDNA template. Amplifications were done using the following cycle settings: 94°C for 30 sec, followed by 35 cycles at 94°C for 15 sec, 54/58°C (according to primer pair) for 15 sec, 72°C for 20 sec. A dissociation curve was systematically generated to confirm the amplification of the PCR single bands. The primer pairs used in this work were those from Lopez et al. (2012). Each pair was verified *in silico* on the JGI genomic dataset (V12.1) from *P. deltoides* (WV94, v2.1) concomitantly to molecular analysis on cDNA and gDNA samples. The amplified fragments had an average size of 200 nucleotides. MIP nomenclature and primers are listed in Supplemental Table S1. The differential state levels of gene expression were calculated from the threshold cycle (CT) and using the formula $2^{-\Delta\Delta C_T}$ according to Livak and Schmittgen (2001). This corresponds to the fold change of an isoform at a given time point relative to its expression from well-irrigated trees, or for daily assessment at their related initial pre-dawn time points (5:00). For each biological sample, each PCR run was performed in duplicate. Negative controls without cDNA were used in all the PCR reactions. To normalize the amount of transcripts present in each reaction, five putative internal controls [*Actin2*, *EF1α*, *SAND*, *TIP41-like* (for type 2A phosphatase activator TIP41), and the *UP2* nomenclatures and primers given in Supplemental Table S1], were chosen from different protein families to reduce the risk of co-regulation. These reference genes were

selected from a number of candidates using the software application BestKeeper (Pfaffl et al., 2004), first to determine the most suitable reference genes from nine widely used housekeeping genes (Czechowski et al., 2005; Xu et al., 2011), and then to estimate a BestKeeper Index used as a calibrator. Lastly, signal intensity data for all transcribed PIP and TIP genes were hierarchically clustered (Ward contrast, Euclidean distance), with R (v3.4.3, R Core Team, 2017) and gplots (v3.0.1, Warnes et al., 2016) libraries.

2.4. In situ *hybridization*

Fresh leaves were harvested, cut and immediately fixed in 4% (w/v) paraformaldehyde + 1 µl/ml triton X-100 for 2 h at 4°C, and the fixation was then extended overnight in 4% PFA alone. Fixed samples were rinsed in PBS (135 mM NaCl, 3 mM KCl, 1.5 mM KH_2PO_4, 8 mM Na_2HPO_4, pH 7.2), then dehydrated and progressively embedded in paraffin (Paraplast, Sigma Aldrich, Saint-Louis, MO, USA) (Brunel et al., 2002). Samples were cut into 10 µm sections with a rotary microtome (HM340E, Microm International GmbH, Walldorf), mounted on Superfrost Plus slides (Fisher Scientific, Elancourt, France) and dried at 42°C for one day for *in situ* mRNA localization. Five gene-specific RNA probes were designed to be located in the variable 3'UTR region of the *PdPIP1;1*, *PdPIP2,4*, *PdPIP2;10*, *PdTIP1;3* and *PdTIP2;1* transcripts with an average size of 200 ribonucleotides (primers detailed in Supplemental Table S1). DNA coding the probes was cloned in *p*GEM® T-Easy vector (Promega®). Sense and antisense probes were synthesized by *in vitro* transcription as described earlier (Brunel et al., 2002), and final detection was as described in Lopez et al., (2016). Observations were made under an Axioplan 2 microscope (Zeiss, Jena, Germany). Data were recorded on a digital camera (AxioCam HR, Zeiss) using Axiovision digital imaging software.

2.5. 3D X-ray microtomography observations

Three-dimensional pictures of the internal structure of *Populus* leaves were acquired using the X-ray microtomographic method (Nanotom 180 XS, GE, Wunstorf, Germany). A minimum of two leaves were sampled at predawn (5:00 am) and midday (2:00 pm) from control and stressed plants. Leaves were dipped in silicone oil to prevent severe dehydration during sample preparation and image acquisition. Small disks were cut in the base of the silicon oil-submerged leaf, at 5 mm from the petiole, including the midrib of the leaf. They were placed in a gelatin capsule (diameter 5 mm and height 1.5 cm, size 4, Euromedex) containing silicone oil. The field of view was ~2.5 × 2.5 × 2.5 mm^3 and covered the full cross section of the disks. X-ray settings were 60 kV and 240 µA. We used a molybdenum target to increase contrast for low-density tissues. For each leaf, 1000 images (250 ms each) were recorded during the 360° rotation of the sample. Full 3D volumes, with a final spatial resolution of 2.5 × 2.5 × 2.5 $µm^3$ per voxel, were reconstructed by Datos x 2.0 (Phoenix,

Nanotom 180 XS, GE, Wunstorf, Germany) software. Volumic image analysis and display, including 2D slice extraction, were performed using VGStudio Max©2.1 software (Volume Graphics, Heidelberg, Germany). After spatial calibration, leaf anatomy was examined by image analysis using ImageJ software. Automatic segmentation enabled the isolation and visualization of the embolized vessels. Indicative leaf water potential was estimated by the mean of Ψ_{leaf} from the two leaves adjacent to those used for the microtomographic analyses, using the Scholander pressure chamber described above. The water potentials indicated on the figure 6AB were provided for information purposes only. Leaf shoots were not equilibrated prior to measurement, generating values of leaf water potentials that can be slightly overstated. Likewise, they do not reflect the water potentials of the disks.

2.6. Statistical analysis

Data for each biological assay are presented as the means ± standard error (SE) of the number of experiments (ecophysiological analyses, n = 7; molecular analyses, n = 3). All quantitative data were processed with STATISTIX V8 software (2012) and using a one-way analysis of variance (ANOVA) followed by a Tukey's honest significant difference (HSD) *post hoc* test ($p < 0.05$). For the principal component analysis (PCA), ecophysiological and molecular data were aggregated. Ecophysiological variables were Ψ_{leaf}, RWC, K_{leaf}, C_{leaf}, E and g_s. Molecular data were *q*PCR expression levels for AQP. The PCA was performed using R software (version 3.4.3, *R*-core Team, 2017) with FactoMineR (v1.39, Le et al., 2008), missMDA (v1.11, Josse and Husson, 2016) and Factoextra (v1.0.5, Kassambara and Mundt, 2017) libraries. Data were scaled to unit variance, and the number of dimensions for the PCA was estimated at 10 by cross-validation.

3. Results and discussion

3.1. Drought impact on leaf hydraulics

Water deprivation is one of the most important factors responsible for down-regulating an array of physiological processes in vascular plants. This down-regulation affects transpiration status, which plays a central role in the systemic regulation of water streams, creating a driving tension in plants from the root system. Our observations on leaf water status, predawn and midday water potential in well-watered plants was -0.05 MPa and -0.8 MPa, respectively (Figure 2A), matching those already reported in balsam poplar (Larchevêque et al., 2011) and black poplar (Lopez et al., 2013). By contrast, in water-depleted poplars, leaf water potential dropped remarkably to -2.6 MPa (Day 7) and beyond (Day 8). These values matched a π_{tlp} value at -1.67 MPa and a RWC_{TLP} of 86% (Supplemental Figure S2) and confirm that *P. deltoides* is among those species with moderate drought tolerance (Bartlett et al., 2012; Garavillon-Tournayre et al., 2017). In this species, Tyree et al. (1992) showed a severe loss of conductivity and 100% embolism at Ψ_{xyl} = -2 MPa. As such, it was suggested that the eastern cottonwood (*P. deltoides*) is among those temperate species most vulnerable to cavitation. As a phenotypic trend characterizing the *Populus* genus, this vulnerability relates to their riparian occurrence and their pioneer species status (Fichot et al., 2015). There is a lack of data available on the leaf water potential in *P. deltoides* under water stress in the field. For most studied species, when the Ψ_{leaf} drops below -3 MPa, there is a loss of turgidity and/or death of all or part of the organ (Blackman et al., 2009); this extreme is observable for *P. deltoides* when Ψ_{leaf} falls below -4 MPa (data not shown).

By Day 6, Ψ_{leaf} started to decline significantly through water deprivation (Figure 2A). Concomitantly, g_s and E started to decline, along with the closure of stomata (Figure 2EF). The tissue dehydration marked by a leaf water potential down to -3.5 MPa (Day 8, Figure 2A) was preceded by a gradual decrease in water flow underlined by drop in stomatal conductance (Day 6, Figure 2F) and reduction of transpiration (Day 6, Figure 2E) as already reported by Smith et al. (1987). Stomatal closure at early dehydration stages would reduce tensions in the transpiration stream, maintaining a minimum plant water potential level that prevents cavitation into the plant vascular system, from roots to leaves. In leaves, several environmental signals (*e.g.* low CO_2, high vapor pressure deficit) can modulate the stomatal closure in relation with the early onset of drying (Bunce, 2006). However, the regulating mechanisms of stomatal closure during dehydration can be questioned given reported uncoupling between turgor loss and subsequent xylem cavitation (Bartlett et al., 2016; Hochberg et al., 2017; Martin-StPaul et al., 2017).

In our work, even before leaves died, the fact that the leaf water potential at turgor loss point (-1.67 MPa) corresponds to a RWC of 86% (that is 14% of leaf dehydration; Day 7; figure 2AB; Supplemental figure S2) and that this leaf water potential rapidly declined further to below -3,5 MPa for 35% dehydration (Day 8), is an important piece of the leaf homeohydry puzzle. The indication that leaves may express safety mechanisms through leaf water storage capacitance is an open question we address in this paper. Generally, leaves from woody plants are not considered as water-storing organs. However, the lack of Ψ_{leaf} decrease at Day 6 (Figure 2A) could be explained by the release of "stored" water from some leaf tissues that remain to be identified (*e.g.* apoplastic compartment, symplastic network from vacuoles, xylemic raw sap flow).

Similarly, possible water redistribution within the lamina may play a substantial role in maintaining stress responsiveness and the integrity of the global metabolism. This protective effect was observed primarily at Day 6 of drought, when g_s, E and K_{leaf} began to decline (Figures 2FEC), while Ψ_{leaf}, RWC and C_{leaf} (Figures 2ABD) remained significantly stable. Once Ψ_{leaf} dropped to around -1.5 MPa, C_{leaf} increased significantly until the turgor loss point was exceeded (-1.67 MPa). It returned to the steady state before stress initiation. These ecophysiological responses reflect, therefore, what we should expect from C_{leaf}. Although activity of certain cellular processes starts to be modulated (or even impaired), C_h could maintain acceptable relative water content in organs to slow down entry into turgor loss (which results in a systemic risk of dehydration symptoms) thereby prolonging the physiological activity of the organs.

The last ecophysiological aspects that need to be studied in correlation with previous leaf traits are the stem diameter variations and the full mass of our experimental system (pot and plant), which together reveal fluctuations in the general plant water status (Steppe et al., 2006; De Schepper et al., 2012). Two significant fluctuations were analyzed: first the diurnal variations in the control plants consecutive to depletion and refilling of internal stem water storage, and second the behavior of plants in a progressive drought process, where the stem diameters and the plant weight consistently dropped with no possible replenishment at night to ensure tissue rehydration (Figure 1). In detail, the water content of the experimental system brutally decreased in an irregular manner, then gradually, after Day 4. This biphasic decline suggests evapotranspiration, followed by residual cuticle transpiration; two physiological processes that act in concert for controlling plant water status and helps plants survive under drought (Javelle et al., 2011). Stem diameters only broke down substantially after Day 6 of drought, and significantly correlate with the onset of K_{leaf}, g_s and E decreases.

To complete this ecophysiological study, during rewatering, Ψ_{leaf} and RWC reverted faster than g_s, E and K_{leaf} to pre-drought hydration levels. This slow recovery of both g_s-E and

hydraulic conductance, when the organs seemed to have secured renewable contents of water pools, could be promoted by an overall gradual hydraulic repair.

3.2. Expression of *PIP* and *TIP* in drought-challenged leaves

It is now widely accepted that the aquaporins (AQP), ubiquitous pore-forming integral membrane proteins, play an essential role in plant-water relations (Prado and Maurel, 2013). In several plant species, multiple AQP isoforms are present ubiquitously in leaf tissues, and their regulation under drought stress and rewatering, notably transcriptional, has pointed to their involvement in leaf hydraulics (Galmés et al., 2007; Pou et al., 2013). However, although the physiological roles of aquaporins in plants have been long debated, many questions remains unanswered. We sought to gain a better understanding of how plasma membrane and tonoplast intrinsic protein genes (*i.e. PIP* and *TIP*, respectively) in drought-challenged *Populus* leaves are modulated, and to what extent these channels are linked to the leaf-water relation.

The *Populus* genome contains 15 PIP members: 5 *PIP1*, 10 *PIP2*, and 17 *TIP* (Gupta and Sankararamakrishnan 2009, Lopez et al., 2012). Based on hierarchical clustering (Figure 3), nearly two-thirds of *PIP* and *TIP* genes (3 *PIP1*, 8 *PIP2* and 12 *TIP*) were constitutively expressed and exhibited differential expression during stress. All of them significantly exhibited differential two-phase responses between water deprivation and recovery (Figure 3 and Supplemental Figures S3-S4). These contrasting expression levels support the function assignment of these isoforms to leaf transcellular water flow. Interestingly, up- and down-regulations occurred in isoform-balanced proportions. Down-regulations concerned *PdPIP1;2-3*, *PdPIP2;6-7*, *PdTIP1;2-5-6-7*, *PdTIP2;1-2*, *PdTIP3;1* and *PdTIP4;1*, and up-regulations concerned *PdPIP1-1*, *PdPIP2;1-2-3-4-10*, *PdTIP1;1-3* and *PdTIP3;2*. Similar modulation of PIP and TIP expression levels during water stress and recovery has been observed in many woody plants such as walnut, grapevine and *Populus* (Sakr et al., 2003; Pou et al., 2013; Secchi et al., 2010; Lopez et al., 2013; Laur and Hacke 2014). Furthermore, the specific expression of *PdPIP2;2* (*PdPIP2;3* and *PdTIP3;2*, to a lesser extent) during recovery suggests that poplar leaves sense rehydration quickly. These molecular findings strengthen the view that recovery from stress should be seen as a specific process and not simply a passive return to the initial steady state.

It is commonly accepted that aquaporins allow transmembrane water movement along osmotic or hydraulic gradients. The fact that a set of AQP is up-regulated during water deprivation suggests that leaves keep a constant fine-tuned balance between water loss and water uptake. However, because drought impedes water uptake, we speculate that a controlled adjustment of the whole AQP pool may occur differentially in various cell/leaf sub-compartments and limit a catastrophic process of tissue death. It is thus of interest to know

how each AQP is involved in adjusting dynamic leaf hydraulic trade-off between main use and storage capacities.

At this stage, we are unable to propose any functional interpretations of AQP isoform steady state levels. The role of the AQP in the regulation of physiological status under hydric constraint is highly complex and still largely unraveled, especially for plant species that share important multigenic families. *Populus*, with 54 AQP (including 15 PIP and 17 TIP), is one such (Secchi et al., 2009; Lopez et al., 2012). The contrasting patterns of expressed isoforms suggest compensating events between isoforms, *i.e.* one AQP group taking over the functions of the isoforms from another group, thus creating differential flow and possibly preferential orientation of water flow. Similarly, the contrasting pattern of isoforms within different AQP sub-families, whichever their expression group (up or down), reveals a complex participation of aquaporins in water flow between cytosol and morphoplasm. They could act in different phases of water deficit and recovery, as for *PdPIP2;4-10* or *PdPIP2;2*, respectively. Unfortunately, the use of transgenic plants or specific mutants cannot provide a clear answer in *Populus*, precisely because such a compensational effect could potentially be produced by several endogenous AQP counterparts.

The AQP expression patterns reveal that their contribution to flow may be relatively complex and highly regulated. To examine the collinearity between transcribed AQP, and between transcribed AQP and ecophysiology variables, a principal component analysis (PCA) was carried out (Figure 4). The first dimension (Dim1) and the second dimension (Dim2) summarized 44.81% and 19.32% respectively of the global variance in the molecular and ecophysiology response curves. Overall, AQP collinearized well with each other and with ecophysiological responses, with the notable exception of C_{leaf}. In addition, the PCA analysis revealed two AQP expression profiles, namely up- or down-regulated (Figure 3). In addition, this PCA offers a useful glimpse of an AQP split that could be detected from hierarchical plotting (Figure 3): one AQP group is essentially made up of TIP subfamily members remarkably correlated with two ecophysiological parameters (g_s-E-K_{leaf} and RWC-Ψ_{leaf}) (on the right part of the figure), and the second of several PIP subfamily members (plus *PdTIP11*) that are clearly anticorrelated to RWC and Ψ_{leaf} (on the left of the figure). There are no previous reports of this balance between TIP and PIP subfamilies during water stress in *Populus*. Regulation of water status is a complicated process, in which PIP and TIP aquaporins can account for the major proportion of the hydraulic conductivity of the plasma membrane and tonoplast, respectively. PIPs take part in a transcellular water transport, whereas TIPs take part in the regulation of water exchange between the cytosolic and vacuolar compartments. During any cell environmental changes, TIP are involved in the fast osmotic adjustments of the cytoplasm, then maintaining general osmolality and cell turgor.

494 Therefore, a fine balance between PIP and TIP subfamilies occurs, where the tonoplast
495 water permeability enables rapid osmotic adjustment in liaison with constant changes in
496 transcellular water flow, where PIPs also fulfill an essential complementary role.

497 Unfortunately, we cannot reasonably speculate on a comparative functional analysis within
498 and between MIP subgroups: TIP and PIP nomenclature is merely historical and does not
499 accurately reflect cell sub-localization, *i.e.* by definition TIP for tonoplast (vacuolar)
500 membrane or PIP for plasma membrane, respectively, knowing that PIP and TIP could be
501 inserted in both these membranes (Gattolin et al., 2011). That reflects a more complex and
502 fine-tuned regulation of aquaporin localization and activity in different physiological contexts.
503 Also, TIP are under-represented in studies of water flow through droughted tissues
504 compared with PIP, so that many questions about this subfamily remain unanswered. The
505 relative importance attached to PIP derives from a presumed dominant role conferred on the
506 plasma membrane in the transcellular pathway of water flow. The main reason for this is that
507 the hydraulic conductivity of the cell membrane is lower than that of the tonoplast membrane
508 (Maurel et al., 1997). Plant cells differ notably from other organisms (*e.g.* fungi, animals or
509 bacteria) in that intracellular spaces are dominated by a central large vacuole; these
510 differential water conductivities could therefore result in a fine-tuned control of water flow
511 from tonoplast to cytosol that minimizes any changes in cytosolic volume during water stress.
512 Previous studies have reported that several differentially expressed AQP genes seem to
513 have a strong impact on organ hydraulics (Chaumont and Tyerman, 2014). Here, PIP and
514 TIP displayed interesting, contrasting correlations that support the general assumption that
515 all these regulations imply assigned functions of several AQP isoforms from various
516 subfamilies. In addition, we assume that behind an apparent isoform abundance from this
517 MIP superfamily, a regulatory framework between counterparts should occur, notably co-
518 expressions with plausible hetero/homo-di/tetramerization events that would potentiate the
519 regulation of their transport activities (Fetter et al, 2004; Zelazny et al., 2007; Secchi and
520 Zwieniecki, 2010). Examining the AQP tissue localization will provide additional information
521 to decipher this intricate regulation network.

522 In previous work, authors report that most of the AQP show a relatively ubiquitous
523 expression in *Populus* (Gupta and Sankararamakrishnan, 2009), but to our knowledge, little
524 information has specifically revealed AQP subtissular distribution in leaves and differential
525 state levels of their expression. *In situ* hybridization (ISH) gave new insights that could help
526 in this respect. Among the 23 transcribed AQPs, we present the localization of five isoforms
527 (Figure 5; Supplemental Figures S5-S6). Interestingly, while *PdPIP2;10*, *PdTIP1;3* seemed to
528 show a rather widespread distribution in leaves, *PdPIP1;1*, *PdPIP2;4* and *PdTIP2;1* exhibited
529 a relative stronger expression in vascular bundles (mainly phloem) and collenchyma cells of

the midrib region. Furthermore, *PdPIP2;4 and PdPIP2;10* showed a more pronounced transcript abundance in the bundle sheath cells (BSCs), a layer of parenchyma cells surrounding the vasculature particularly visible from the second-order veins in *P. deltoides*, when staining for *PdTIP2;1* was confined essentially to cells nearest the vascular system and was near-absent for *PdTIP1;3* in the whole of the BSC territory. These findings are highly significant because these mRNA over-accumulations in AQP, which are more predominant in all peripheral extraxylar vein tissues, are in line with the functional role of the extraxylary veins and BSCs in the regulation of the leaf radial transport of water by acting as a xylem-mesophyll hydraulic barrier, a mechanism that implies AQP activity (Sade et al., 2014; Prado et al., 2013).

But what is probably even more interesting would be to integrate AQP in a complex of integral membrane proteins that acts in the cell sensing. In drought, cells experience turgor loss with an induced membrane shrinkage that could activate mechano- hydro- and osmo-sensing channels or proteins: in mammals, AQP5 has been shown to interact with volume-sensitive ion channels, indicating AQP involvement in cell volume sensing (Liu et al., 2006). In water challenged leaves, and particularly in the mesophyll cells and the bundle sheath cells, we could expect that differential threshold water potentials could trigger specific hydrostimulus responses, which are still not understood. Could the protective responses of capacitance then be a compromise between hydromechanical stimulus and physiological influences where AQP and various partners act in concert?

Highly challenging areas for research are thus highlighted here: the spectrum of specific MIP subfamilies involved in the physiological leaf responses to depletion and refilling of internal stem water storage as well as their potential functional sub-compartmentalization in the leaves remain to be elucidated.

3.3. Water storage, extraxylem territories and AQPs

The extraxylem pathway, and in particular the bundle sheath cells (BSCs), appears to play a special role in regulating leaf water movements from vasculature to epidermis (Buckley et al., 2015; Caringella et al., 2015; Ohtsuka et al., 2017). Furthermore, it is reported that AQP regulate the water flow across cell membranes (Heinen et al., 2009; Shatil-Cohen et al., 2011; Laur and Hacke 2014). Yet there is still a lack of knowledge on leaf water storage, particularly in woody perennial organisms such as *Populus*. Micro-CT imaging provided detailed spatial information about leaf sub-structure and related hydric status: most water- and gas-filled conduits (phloem, xylem) and parachymal areas *lato sensu* (veins and lamina) were clearly distinguishable, appearing filled or empty (light or dark gray, respectively). In the present study, the level of embolized vessels is only qualitatively discussed because a

quantitative evaluation of this phenomenon remains uncertain on excision of small organs that are under strong hydraulic tensions and there is always a risk of overestimating the xylem embolism in the samples (Wheeler et al., 2013). Similarly, we cannot monitor the hydration level of the different leaf tissues. Lastly, the water potentials displayed on the figure 6AB are only indicative and correspond to the mean of the Ψ_{leaf} from the leaves adjacent to those used for the microtomographic analyses.

However, our analysis showed a remarkably contrasting sub-tissular distribution of the water contents within a severely water-challenged leaf (Ψ_{leaf} < -2.5 MPa) compared with a well-hydrated one (Figure 6AB). Xylem vessels appear highly embolized, and the spongy mesophyll tissue in lamina appears to be dried out (cell shrinkage events resulting from possible cell necrosis and/or intercellular spaces being emptied of water). That contrasts with the cell structure in the leaf peripheral extraxylar vein tissues that seems to exhibit any significant variation; this applies to all living tissues, *i.e.* phloem, sclerenchyma, parenchyma and collenchyma cells. It is reasonable to assume that as any leaf tissues under severe drought constraint, these territories undergo the decreasing phases of water status. However, they exhibit relatively strong water retention efficiency. But even more interesting, the analysis of these territories draws special attention to BSC. In many dicotyledons, including *Populus*, the bundle sheath of secondary and minor veins extends towards the epidermis forming a bundle sheath extension (BSE) that separates the leaf into specialized compartments. It has been suggested that such leaves, referred to as heterobaric leaves, are an adaptation for retaining water and protecting the mesophyll against drought stress (Terashima, 1992). Bulk mesophyll cells only seems to suffer slight changes in water potential and influence the dynamics of K_{leaf} in response to irradiance and leaf water status (Sommerville et al., 2012; Sack and Scoffoni, 2013), as well as to stomatal control (Rockwell and Holbrook, 2017). However, incorporating BSC in a protective scheme against overall leaf dehydration as previously suggested by Griffiths et al. (2013) is still not simple as it is now increasingly accepted that there is relatively little dehydration of this tissue during an extreme drought. These BSC may be potential water stores or capacitors that are elicited in much more extreme drought conditions. The paradox is that leaves are already at the limit of hydraulic dysfunction, and have, therefore, gone into survival mode.

Tissue shrinkage and xylem embolism depend on the water potential of a plant challenged by multiple environmental contexts. Physiologically, a sustained period of drought is highly hazardous for plant integrity in general, but even more so for leaves because of their structure and position on trees. Leaves endure continuous changes in their hydric status, which conditions cell metabolic activity. In the event of drastic decline in leaf water potential, general metabolic performance depresses and there is an considerable emergence of “waterless holes” throughout the spongy mesophyll (major leaf metabolic scene).

Admittedly, leaves are the seat of photosynthesis, one of the most remarkable bioengineering processes in the whole living world in which light energy is used to make sugar. And so viewing leaves from deciduous trees as possible water capacitors is uncommon, and therefore not a trivial matter. Yet, at the tissue level, persistent water contents support the hypothesis that veins could act as a water storage network. However, if a certain volume of water can be stored in veins (and possibly in BSC), how might the leaves then benefit from it? Likewise, what are the regulatory mechanisms of the cell that enable them to take water from the immediate cell environment, store it in possibly unfavorable contexts of water potential and, if necessary, redistribute it in some way and that, to what extent (the essence of all storage)? These issues obviously require further attention.

The aquaporins might offer one way to help address these questions. In a context where the BSEs radial apoplast pathway of water and the passive water diffusion through cell membranes are near-negligible, the water reallocations and/or retentions that occur by expected modulation of the hydraulic resistance of cells have to be acutely controlled. In this context, along with additional and modulated molecular events such as suberin and lignin depositions in cell walls (Mertz and Brutnell, 2014; Ohtsuka et al., 2017) or osmolyte accumulations (Williams et al., 1993), there is a strong presumption that leaf aquaporins are involved in the regulation of the water supply from the xylem to the peripheral extraxylar veins towards all of the extravascular compartments and the subsequent limb (Sack and Holbrook, 2006; Lee et al., 2009; Shatil-Cohen et al., 2011). ISH suggests a sequential allocation of different AQP members as the relay between the various leaf sub-territories, which ensure a compartmentalized water distribution (Figure 5). Suitable modulations of AQPs could thus co-design the hydraulic network architecture of transient water sources (or reservoirs such as the peripheral extraxylar area) and sinks (lamina), and thereby, be the trade-off between the capacitance and conductance processes. This hydraulic argument is strengthened by the joint examination of X-ray microtomography (Figure 6AB) and ISH outcomes (Figure 5), two complementary methodologies.

To our knowledge, this is the first time this biological demonstration has been provided clearly. Figure 6C presents a schematic diagram, based on the electric circuit analogy, showing the hydraulic model of water flow in leaves. It depicts the relationships between the hydraulic resistances (*R*) and the AQP (one of the molecular mechanisms of this resistance), and the hydraulic capacitances (*C*), which regulate the balance in water diffusion and storage between leaf sub-territories.

4. Conclusion

Although a small fraction of daily transpiration is generally attributed to water stored in leaves, the present study reveals the existence of several water storage compartments that

could act as water potential buffers, damping variations in leaf xylem. This phenomenon pertains to the phloem and all the peripheral networks within the veins. The protective effect may be regulated by the activity of aquaporins localized in the surrounding regions of leaf vascular bundles, as some AQP members are differentially expressed with a contrasting tissue-dependent pattern under drought and recovery conditions. Knowing the contribution of each isoform in each leaf reservoir would provide more information about the regulation of leaf hydraulic conductivity and capacity along the radial xylem-to-mesophyll pathway and *vice versa* as a water-saving and drought-escaping mechanism.

Despite the volume of studies on leaf responses to water stress, many unanswered questions linger. The diversity of the underlying mechanisms (*e.g.* ecophysiological, anatomic, chemical and molecular) involved in the regulation of the leaf turgor maintenance makes fully understanding water regulation by its molecular actors even more of a challenge. These molecular ecophysiological findings highlight original observations, and further research will now be needed to unravel the biological significance and the regulation levels of the stress-strength-dependent dynamic water movement and storage observed in *Populus* leaves.

ACKNOWLEDGEMENTS

This work was supported by the European Community's Seventh Framework Program [FP7/2007-2013; FP7-PEOPLE-2011-IEF / proposal No. 303059]. We are grateful to two anonymous reviewers for improving the manuscript.

AUTHOR CONTRIBUTIONS STATEMENT

Beatriz MURIES co-designed and participated in all the experiments, and wrote the first draft of the article;

Robin MOM, Pierrick BENOIT participated in the field experiments, and acquisition of ecophysiological data;

Nicole BRUNEL-MICHAC supervised ISH experiments;

Patricia DREVET, Gilles PETEL, Boris FUMANAL, Aurélie GOUSSET-DUPONT, Hervé COCHARD, Eric BADEL, Jean-Louis JULIEN, Philippe LABEL, and Daniel AUGUIN made a critical examination of the manuscript;

Jean-Stéphane VENISSE led the program, co-designed the experiments, obtained the funding, and coordinated and compiled the authors' contributions to the final version of the article. He wrote the final draft of the article and edited it.

All the authors participated in the analysis of data, and collectively approved all the interpretations of results and related hypotheses.

Captions

Figure 1. Daily variations in the experimental system weight (pot and plant) (black line; kg; analytical balance) and stem diameter (gray line; µm; LVDT) of *Populus deltoides* in different hydric conditions: well-watered (dark blue), drought treatment (orange, monitored over 8 days), and rewatered (light blue, monitored over 10 days). Curves are representative of one tree. Detail in the typical time courses of diurnal variations of experimental system weight and stem diameter in Supplemental Figure S1.

Figure 2. Water relation parameters [(**A**), Ψ_{leaf}, leaf water potential ; (**B**), RWC, relative water content ; (**C**), leaf hydraulic conductance, K_{leaf} ; (**D**), leaf capacitance, C_{leaf}], and gas exchange parameters [(**E**), transpiration flux, E ; (**F**), stomatal conductance, g_s] in well-irrigated plants (dark blue curves), drought treatment (orange curves) and rewatering (light blue curves). Ecophysiological traits were recorded at predawn (5:00 am) and midday (14:00 pm). na: g_s non-available data. Data correspond to the mean of seven independent biological experiments. Bars represent the biological standard error. Letters on vertical bars indicate significant differences between treatments [Tukey *post hoc* test after one-way analysis of variance (ANOVA), $p < 0.05$].

Figure 3. Hierarchical clustering of all PIP and TIP transcribed in *Populus deltoides* and transcriptional accumulation patterns of a selected set of *PdPIPs* and *PdTIPs* in leaves of plants challenged by a drying-rewatering cycle. All expressed PIPs and TIPs are shown in Supplemental Figures S3 and S4, respectively. Molecular analyses were performed at predawn (5:00) and midday (14:00). Transcript levels for each gene were estimated using real-time qRT-PCR analyses and normalized by the expression of five housekeeping genes. Relative transcript abundance rates were obtained by the $2^{-\Delta\Delta C_T}$ method with transcript abundances. Data correspond to means of three independent biological replicates. Bars represent the biological standard error. Data not sharing the same letters are significantly different [Tukey *post hoc* test after one-way analysis of variance (ANOVA), $p < 0.05$]. Genes were clustered by a hierarchical clustering algorithm (green, up-expression; red, down-expression, compared with untreated samples). Hierarchical clustering was performed by similarity on $\log_2$ signal intensity data, and calculated according to Euclidean distance with Ward contrast between expression levels of all PIP and TIP genes (R). Well-watered plants, dark blue; droughted plants, orange; rewatered plants, light blue.

Figure 4. Principal component analysis based on the ecophysiological data (gs, Ψ_{leaf}, C_{leaf}, E, K_{leaf} and RWC) and molecular data (PIP and TIP qPCR expression levels). PCA was

performed using FactoMineR_1.39, missMDA_1.11 and Factoextra libraries (*R* software; version 3.4.3; *R*-core Team, 2017). PSI, Ψ_{leaf} for leaf water potential ; RWC, relative water content ; C_{leaf}, leaf capacitance ; g_s, leaf stomatal conductance ; *E*, transpiration flux ; K_{leaf}, leaf conductance ; PIP, plasma intrinsic protein ; TIP, tonoplast intrinsic protein. TIP and PIP nomenclatures used here are contractions in the first and second numbers preceded by the AQP subfamily type, each contraction corresponds to a specific isoform (for example, PIP11 for *Pd*PIP1;1, etc).

Figure 5. *In situ* localization of selected *PdPIP* and *PdTIP* in midrib (**A**, **D**, **G**, **J**, **M**), lamina (**B**, **E**, **H**, **K**, **N**) and BSCs (**C**, **F**, **I**, **L**, **N** ; extracted from **B, E, H, K, N**) of the leaves from *Populus deltoides*. Pictures correspond to paraffin-embedded transversal sections of leaf samples hybridized with specific antisense probes (i.e. positive, +). Paraffin-embedded transversal sections of leaf samples hybridized with specific sense probes (i.e. negative controls, -) are presented in Supplemental Figure S5. Positive hybridization signals are visualized by violet staining using a DIG-labeled RNA immunodetection system. Arrows indicate differential hybridizations (+ *vs* -). co, collenchyma ; pa, parenchyma ; co-pa, collenchyma and parenchyma (structures not distinguishable individually) ; ca-ph, cambium and phloem (structures not distinguishable individually) ; sc, sclerenchyma ; pal, palissadic parenchyma of lamina ; sp, spongy parenchyma of lamina ; mv, minor vein used to describe BSC (**C**, **F**, **I**, **L**, **N**) ; BSC, bundle sheath cells ; xy-ph, xylem and phloem (structures not distinguishable individually). Leaf anatomical features are detailed in Supplemental Figure S6. Bar indicates 100 µm.

Figure 6. *In vivo* visualization by X-ray microtomography of tissue embolism in a leaf from *Populus deltoides*. Reconstructed cross sections showing embolized (dark points) midrib and vein conduits, and lamina at leaf water potential around (**A**) -0.05 MPa (control sample), (**B**) <-2.5 MPa (drought sample). These water potentials correspond to the mean of Ψ_{leaf} from leaves adjacent to those sampled at 5:00 am for X-ray microtomography analysis. Bar indicates 100 µm. Leaf anatomical features are detailed in Supplemental Figure S6. The leaf in (**B**) was especially sampled for quantitative illustration, highlighting potential wilting symptoms induced by drought just before rewatering. (**C**) Leaf hydraulic model of water flow based on the electric circuit analogy depicts the relationships between hydraulic resistances (*R*) and the hydraulic capacitances (*C*) that regulate the balance in water diffusion and storage through different leaf areas when leaf water potential (ψ_{leaf}) is below -2,5 MPa corresponding to severe drought. Downward- and upward-pointing red arrows represent down- and up-regulation, respectively. Line size for "*R* and *C* hydraulic components" represents the intensity of their involvement in the hydraulic system. Aquaporins are shown

in yellow by their tertiary structure, and their size represents their presence assessed by ISH. Marked AQP in the "xylem" box indicate that they are absent in secondary xylem. g_S, stomatal conductance; pal, palissadic parenchyma; col, collenchyma; bsc, bundle sheath cell; mv, minor vein.

Supplemental Figure S1. Detail in the typical time courses of diurnal variations of experimental system weight (black line) and stem diameter (gray line) of *Populus deltoides* under full irrigation, in correlation with the photosynthetic active radiation (red line) on day 2 of treatment. The experimental design shows the time of molecular sampling and ecophysiological recording (at 5:00 and 14:00), and the watering pulse (well-watered plants in dark blue) and the end of irrigation to start of drought treatment (unwatered plants in orange).

Supplemental Figure S2. (**A**) Changes in the leaf water potential (Ψ_{leaf}) in relation with the leaf capacitance (C_{leaf}). This representation was generated from the Höfler diagram (**B**), which shows the changes in whole leaf water potential (Ψ_{leaf}), pressure potential (P_{leaf}) and osmotic potential (π_{leaf}) as a function of relative water content (RWC). TLP, turgor loss point.

Supplemental Figure S3. Transcriptional accumulation patterns of all *PdPIPs* in leaves of plants challenged by a drying-rewatering cycle. Transcript levels for each gene were estimated using real-time *q*RT-PCR analyses and normalized by the expression of five housekeeping genes. Relative transcript abundance rates were obtained by the $2^{-\Delta\Delta C_T}$ method with transcript abundances. Data correspond to means of three independent biological replicates. Bars represent the biological standard error. Data not sharing the same letters are significantly different [Tukey *post hoc* test after one-way analysis of variance (ANOVA), $p < 0.05$]. Well-watered plants, dark blue; droughted plants, orange; rewatered plants, light blue.

Supplemental Figure S4. Transcriptional accumulation patterns of all *PdTIPs* in leaves of plants challenged by a drying-rewatering cycle. Transcript levels for each gene were estimated using real-time qRT-PCR analyses and normalized by the expression of five housekeeping genes. Relative transcript abundance rates were obtained by the $2^{-\Delta\Delta C_T}$ method with transcript abundances. Data correspond to means of three independent biological replicates. Bars represent the biological standard error. Data not sharing the same letters are significantly different [Tukey *post hoc* test after one-way analysis of variance (ANOVA), $p < 0.05$]. Well-watered plants, dark blue; droughted plants, orange; rewatered plants, light blue.

Supplemental Figure S5. *In situ* localization of a selected *PdPIP* and *PdTIP* in midrib and lamina of a leaf from *Populus deltoides*. Photographic images with letters correspond to Figure 5. Paraffin-embedded transversal sections of leaf samples hybridized with specific antisense probes (*i.e.* positive, +) or with sense probes as negative controls (-). Positive hybridization signals are visualized by violet staining using a DIG-labeled RNA immunodetection system. Bar indicates 100 µm. Leaf anatomical features are detailed in Supplemental Figure S6.

Supplemental Figure S6. (**A**) Midrib cross-section and (**B**) anatomic detail of a minor vein within the lamina of a leaf from *Populus deltoides* by light microscopy and toluidine blue staining. (**A**) ue, upper epidermis ; le, lower epidermis ; co, collenchyma ; pa, parenchyma ; xy2, secondary xylem ; xy1, primary xylem (metaxylem and protoxylem not distinguishable) ; ca, cambium ; ph2, secondary phloem (metaphloem and protophloem not distinguishable) ; sc, sclerenchyma ; mv, minor vein. xy2-xy1 transport the xylem sap ; xylem sap-ca-ph2 constitute the vessel tissue (*i.e.* vascular bundle) ; sc-pa-co-le/ue constitute the extravessel tissue ; sap vessel tissue-extravessel tissue constitute the midrib. (**B**) ue, upper epidermis ; pal, palissadic parenchyma of lamina ; sp, spongy parenchyma of lamina ; bsc, bundle sheath cells (area delimited by the red line) ; xy/ph, xylem/phloem (structures individually not distinguishable).

Supplemental Table S1. Primers used for qPCR amplification and the MIP transcript tissue locations using *in situ* hybridization.

	Locus name *Populus deltoides* WV94 v2.1	Primer sequences Forward	Reverse
Actine 2	Podel.19G009700.1	GAAGTGCTTCTAAGTTCTACAAG	CTCAATAAATTCTCCATATCAACC
EF1α	Podel.08G051800.1	GTCTGTTGAGATGCACCACG	CAATGTGACAGGTGTGGCAG
SAND	Podel.09G012400.1	CATGATAAAGGCAACGGGGCG	CTGTGTTACAAGATATTTTTGGG
TIP41-like	Podel.01G317800.1	CAGTGAAAGTGCAAATCCTATTG	CTTACAAGTTACTGTGGACCAC
UP2	Podel.02G140600.1	TATCGTCTTGTGACAATTTTTAG	GGAAGTCCTGGCGCTAATGA
PdPIP1;1	Podel.08G080400.1	CAAGAAGTGATGAYTGTGATGC	ACGTCACTGTTATAGCACGC
PdPIP1;2	Podel.03G137600.1	TTCAAGAGCAGAGCTTAATTTC	TTCAAAAAGCTAGATAATTTACAC
PdPIP1;3	Podel.10G194700.1	AAGAAGTGATTATTATGATTATGG	GATTTGAAGAAACACGTATTGCTA
PdPIP2;1	Podel.09G141800.1	TGCTAACATGGTGGCTCCC	GATCATCCCAGGCTTTCTTATC
PdPIP2;2	Podel.04G178700.1	TGGTACACTTGGCCACAATC	GCTAATGCTCCCACAAATGG
PdPIP2;3	Podel.16G093500.1	ATTCAGTTATGGAACGTACGC	AGCTCACAACCATGACATAAC
PdPIP2;4	Podel.10G227600.1	CCAACGGTTTTAAATCTCGGTTC	ACCGAAAGGGATAATAAAGGG
PdPIP2;5	Podel.06G138200.1	TGTGTACATTATGGTGTCGTG	CAAAGAAGCAGCACTACCTGAGAC
PdPIP2;6	Podel.08G048200.1	ATCCCAATCACAGGAACTGG	CTATGGCTGCACCAATGAAG
PdPIP2;7	Podel.09G012100.1	ATGACCATTGGCTCTTCTGG	GGCTTTAAGCATTGCTCCTG
PdPIP2;8	Podel.05G122300.1	GCAATCCTACTAGCTAAGGC	ACCCACATATCAAGTTGAGAC
PdPIP2;9	Podel.05G122200.1	ACTGGAACTGGCATCAATCC	CCAACCCAGAAAATCCACAG
PdPIP2;10	Podel.06G138300.1	CACAGTCGTGGTCAAGATGTC	ACTAGTTGATTATGAGATAGGGAG
PdTIP1;1	Podel.01G246100.1	TGCTGCCATTGTCTACGAGGTCAT	CACCACCACAGACGTGTCTTC
PdTIP1;2	Podel.09G026800.1	TGCTGCCATTGTCTACGAGGTCTG	AACAACACCAACATCATCCAAACC
PdTIP1;3	Podel.10G214800.1	GATTGGAAACTCCAGCTTTTGGAT	AATTTCCCTTCTTTGGATCCACT
PdTIP1;4	Podel.08G061500.1	ATTGGAAACACCAGCTTTTGGGC	AATTTCCCTTCTTCGGATCCACC
PdTIP1;5	Podel.16G102900.1	ATTGTGGGTGCTAACATTCTAGTC	CCACCAACCAGTGGTCCGGC
PdTIP1;6	Podel.06G131300.1	CAACCACTGGGTCTACTGGGCA	GAAAGAAAAAGCCGCGGCACTG
PdTIP1;7	Podel.09G003500.1	CGAGTTAATCTTCATCAGCCACAC	GGAAAAAATTCAACGTAGTCTTAAAC
PdTIP1;8	Podel.04G222000.1	AGCTTATCTTCATGAGCCACAGTAC	ACGAATCCAACGTAGTCCAAACG
PdTIP2;1	Podel.01G197500.1	TCTACTGGGCTGGGCCTCTTG	CAAGTGAAGTTATTAGAAGTCTCC
PdTIP2;2	Podel.07G052500.1	TCTACTGGGTTGGGCCTCTTA	ATTTTAGACTGACTTAGAACTCATA
PdTIP2;3	Podel.03G081200.1	TTGCTTCAGGGATGAGTGCTATC	TTCAGAAACTGGGGCAGGCGC
PdTIP2;4	Podel.01G168400.1	TCGCTTCAGGGATGAGTGCTGTT	TTCGGAAACTGGGGCAGCGGT
PdTIP3;1	Podel.18G157700.1	GAGCATTTGGGCCTGCTCTAG	GGTGAGCTACTGGCTCTGCTG
PdTIP3;2	Podel.17G170600.1	GAGCTTTTGGGCCTGCTTTAA	GGCGAGGTACTGGCTCTGTGG
PdTIP4;1	Podel.06G131300.1	ATGGGCTAGGTCCAATGCTGAC	GAAGAGGACGATGAGATCTTGTG

References

Aasamaa, K., Sober, A., 2001. Hydraulic conductance and stomatal sensitivity to changes of leaf water status in six deciduous tree species. Biologia Plantarum 44, 65-73.

Aasamaa, K., Sober, A., Rahi, M., 2001. Leaf anatomical characteristics associated with shoot hydraulic conductance, stomatal conductance and stomatal sensitivity to changes of leaf water status in temperate deciduous trees. Australian Journal of Plant Physiology 28, 765-774.

Anderberg, H.I., Kjellbom, P., Johanson, U., 2012. Annotation of *Selaginella moellendorffii* major intrinsic proteins and the evolution of the protein family in terrestrial plants. Frontiers in Plant Science 3: 33.

Attia Z., Domec, J.C., Oren, R., Way, D.A., Moshelion, M., 2015. Growth and physiological responses of isohydric and anisohydric poplars to drought. J. Exp. Bot. 66, 4373-4381.

Bartlett, M.K., Scoffoni, C., Sack, L., 2012. The determinants of leaf turgor loss point and prediction of drought tolerance of species and biomes: a global meta-analysis. Ecology Letter 15, 393-405.

Bartlett, M.K., Klein, T., Jansen, S., Choat, B., Sack, L., 2016. The correlations and sequence of plant stomatal, hydraulic, and wilting responses to drought. Proc Natl Acad Sci USA 113, 13098-13103.

Begg, J.E., Turner, N.C., 1970. Water potential gradients in field tobacco. Plant Physiology 46, 343-346.

Ben Baaziz, K., Lopez, D., Rabot, A., Combes, D., Gousset, A., Bouzid, S. et al., 2012. Light-mediated K_{leaf} induction and contribution of both the PIP1s and PIP2s aquaporins in five tree species: walnut (*Juglans regia*) case study. Tree Physiol. 32, 423-434.

Blackman, C.J., Brodribb, T.J., Jordan, G.J., 2009. Leaf hydraulics and drought stress: response, recovery and survivorship in four woody temperate plant species. Plant, Cell and Environment. 32, 1584-1595.

Brodribb, T.J., Skelton, R.P., McAdam, S.A.M., Bienaimé, D., Lucani, C.J., Marmottant, P., 2016a. Visual quantification of embolism reveals leaf vulnerability to hydraulic failure. New Phytologist 209, 1403-1409.

Brodribb, T.J., Bienaimé D., Marmottant, P., 2016b. Revealing catastrophic failure of leaf networks under stress. PNAS 113, 4865-4869.

Brunel, N., Leduc, N., Poupard, P., Simoneau, P., Mauget, J.C., Viemont, J.D., 2002. KNAP2, a class I KN1-like gene is a negative marker of bud growth potential in apple trees

(*Malus domestica* [L.] Borkh.). Journal of Experimental Botany 53, 2143-2149.

Buckley, T.N., John, G.P., Scoffoni, C., Sack, L., 2015. How does leaf anatomy in fluence water transport outside the xylem? Plant Physiology 168, 1616-1635.

Bunce, J.A., 2006. How do leaf hydraulics limit stomatal conductance at high water vapour pressure deficits? Plant Cell Environ 29, 1644-1650.

Caringella, M.A., Bongers, F.J. Sack, L., 2015. Leaf hydraulic conductance varies with vein anatomy across *Arabidopsis thaliana* wild-type and leaf vein mutants. Plant, Cell & Environment 38, 2735-2746.

Chang, S.J., Puryear, J., Cairney, J., 1993. A simple and efficient method for isolating RNA from pine trees. Plant Mol. Biol. Rep. 11, 113-116.

Chaumont, F., Tyerman, S.D., 2014. Aquaporins: highly regulated channels controlling plant water relations. Plant Physiology 164, 1600-1618.

Choat, B., Jansen, S., Brodribb, T.J., et al, 2012. Global convergence in the vulnerability of forests to drought. Nature 491, 752-755

Czechowski, T., Stitt, M., Altmann, T., Udvardi, M.K. and Scheible, W.R., 2005 Genome-wide identification and testing of superior reference genes for transcript normalization in Arabidopsis. Plant Physiol. 139, 5–17.

Danielson, J.A.H., Johanson, U., 2008. Unexpected complexity of the aquaporin gene family in the moss *Physcomitrella patens*. BMC Plant Biology 8, 45-60.

De Schepper, V., van Dusschoten, D., Copini, P., Jahnke, S., Steppe, K. 2012. MRI links stem water content to stem diameter variations in transpiring trees. Journal of Experimental Botany 63, 2645-2653.

Dobra, J., Motyka, V., Dobrev, P., Malbeck, J., Prasil, I.T., Haisel, D., Gaudinova, A., Havlova, M., Gubis, J., Vankova, R., 2010. Comparison of hormonal responses to heat, drought and combined stress in tobacco plants with elevated proline contents. Journal of Plant Physiology 167, 1360-1370.

Fetter, K., Van Wilder, V., Moshelion, M., Chaumont, F., 2004. Interactions between plasma membrane aquaporins modulate their water channel activity. Plant Cell 16, 215-228.

Ferrio, J.P., Pou, A., Florez-Sarasa, I., Gessler, A., Kodama, N., Flexas, J., Ribas-Carbo, M., 2012. The Peclet effect on leaf water enrichment correlates with leaf hydraulic conductance and mesophyll conductance for CO_2. Plant Cell and Environment 35, 611-625.

895 Fichot, R., Brignolas, F., Cochard, H., Ceulemans, R., 2015. Vulnerability to drought-induced
896 cavitation in poplars: synthesis and future opportunities. Plant Cell Environ 38, 1233-1251.

897 Garavillon-Tournayre, M., Gousset-Dupont, A., Gautier, F., Benoit, P., Conchon, P., Souchal,
898 R., Lopez, D., Petel, G., Venisse, J.S., Bastien, C., Label, P., Fumanal, B., 2017. Integrated
899 drought responses of black poplar: how important is phenotypic plasticity?, Physiologia
900 Plantarum, 163, 30-44.

901 Galmés, J., Pou, A., Alsina, M.M., Tomas, M., Medrano, H., Flexas, J., 2007. Aquaporin
902 expression in response to different water stress intensities and recovery in Richter-110 (*Vitis*
903 sp.): relationship with ecophysiological status. Planta 226, 671-681.

904 Gattolin, S., Sorieul, M., Frigerio, L., 2011. Mapping of tonoplast intrinsic proteins in maturing
905 and germinating *Arabidopsis* seeds reveals dual localization of embryonic TIPs to the
906 tonoplast and plasma membrane. Molecular Plant. 4, 180-189.

907 Griffiths, H., Weller, G., Toy, L.F.M., Dennis, R.J., 2013. You're so vein: Bundle Sheath
908 physiology, phylogeny and evolution in C3 and C4 plants. Plant, Cell & Environment 36, 249-
909 261.

910 Gupta, A.B., Sankararamakrishnan R., 2009. Genome-wide analysis of major intrinsic
911 proteins in the tree plant *Populus trichocarpa*: characterization of XIP subfamily of
912 aquaporins from evolutionary perspective. BMC Plant Biology 20, 134.

913 Heckwolf, M., Pater, D., Hanson, D.T., Kaldenhoff, R., 2011. The *Arabidopsis thaliana*
914 aquaporin *At*PIP1;2 is a physiologically relevant CO_2 transport facilitator. The Plant Journal
915 67, 795-804.

916 Heinen, R.B., Ye, Q., Chaumont, F., 2009. Role of aquaporins in leaf physiology. Journal of
917 Experimental Botany 60, 2971-2985.

918 Heymann, J.B., Engel, A., 1999. Aquaporins: phylogeny, structure, and physiology of water
919 channels. News Physiol Sci 14, 187-193.

920 Hochberg, U., Bonel, A.G., David-Schwartz, R., Degu, A., Fait, A., Cochard, H., Peterlunger,
921 E., Herrera, J.C., 2017. Grapevine acclimation to water deficit: the adjustment of stomatal
922 and hydraulic conductance differs from petiole embolism vulnerability. Planta 245, 1091-
923 1104.

924 Hochberg, U., Windt, C.W., Ponomarenko, A., Zhang, Y.J., Gersony, J., Rockwell, E.F.,
925 Holbrook, N.M., 2017. Stomatal Closure, Basal Leaf Embolism, and Shedding Protect the
926 Hydraulic Integrity of Grape Stems. Plant Physiology 174, 764-775.

927 Jackson, M.B., Saker, L.R., Crisp, C.M., Else, M.A., Janowiak, F., 2003. Ionic and pH

928 signalling from roots to shoots of flooded tomato plants in relation to stomatal closure. Plant
929 and Soil 253, 103-113.

930 Javelle, M., Vernoud, V., Rogowsky, P.M., Ingram, G.C., 2011. Epidermis: the formation and
931 functions of a fundamental plant tissue. New Phytol. 189, 17-39.

932 Josse, J., Husson, F., 2016. missMDA: A Package for Handling Missing Values in
933 Multivariate Data. Analysis. Journal of Statistical Software, 70, 1-31.

934 Kassambara, A., Mundt, F., 2017. factoextra: Extract and Visualize the Results of
935 Multivariate Data Analyses. R package version 1.0.5. https://CRAN.R-
936 project.org/package=factoextra

937 Khan, S.H., Ahmad, N., Ahmad, F., Kumar, R., 2010. Naturally Occurring Organic
938 Osmolytes: From Cell Physiology to Disease Prevention IUBMB Life 62, 891-895.

939 Koide, R.T., Robichaux, R.H., Morse, S.R., Smith, C.M., 1989. Plant water status, hydraulic
940 resistance and capacitance. In Plant Physiological Ecology: Field Methods and
941 Instrumentation (eds R.W. Pearcy, J.R. Ehleringer, H.A. Mooney & P.W. Rundel), pp. 161-
942 183. Chapman and Hall, New York, NY, USA.

943 Larchevêque, M., Maurel, M., Desrochers A., Larocque, G.R., 2011. How does drought
944 tolerance compare between two improved hybrids of balsam poplar and an unimproved
945 native species? Tree Physiology 31, 240-249.

946 Laur, J., Hacke, U.G., 2014. Exploring Picea glauca aquaporins in the context of needle
947 water uptake and xylem refilling. New Phytologist 203, 388-400.

948 Le, S., Josse, J., HussonF., 2008. FactoMineR: An R Package for Multivariate Analysis.
949 Journal of Statistical Software 25, 1-18.

950 Lee, S.J., Murphy, C.T., Kenyon, C., 2009. Glucose shortens the life span of *C. elegans* by
951 downregulating DAF-16/FOXO activity and aquaporin gene expression. Cell Metab. 10, 379-
952 391.

953 Livak, K.J., Schmittgen, T.D., 2001. Analysis of relative gene expression data using real-time
954 quantitative PCR and the $2^{-\Delta\Delta CT}$ method. Methods 25, 402-408.

955 Liu, X., Bandyopadhyay, B., Nakamoto, T., Singh, B., Liedtke, W., Melvin, J.E., Ambudkar, I.
956 2006. A role for AQP5 in activation of TRPV4 by hypotonicity: concerted involvement of
957 AQP5 and TRPV4 in regulation of cell volume. J Biol Chem. 281, 15485-15495.

958 Lopez, D., Bronner, G., Brunel, N., Auguin, D., Bourgerie, S., Brignolas, F., Carpin, S.,
959 Tournaire-Roux, C., Maurel, C., Fumanal, B., Martin, F., Sakr, S., Label, P., Julien, J.L.,
960 Gousset-Dupont, A., Venisse, J.S., 2012. Insights into Populus XIP aquaporins: evolutionary

961 expansion, protein functionality, and environmental regulation. Journal of Experimental
962 Botany 63, 2217-2230.

963 Lopez, D., Venisse, J.S., Fumanal, B., Chaumont, F., Guillot, E., Daniels, M.J., Cochard, H.,
964 Julien, J.L., Gousset-Dupont, A., 2013. Aquaporins and Leaf Hydraulics: Poplar Sheds New
965 Light. Plant Cell Physiology 54, 1963-1975.

966 Lopez, D., Amira, M.B., Brown, D., Muries, B., Brunel-Michac, N., Bourgerie, S., Porcheron,
967 B., Lemoine, R., Chrestin, H., Mollison, E., Di Cola, A., Frigerio, L., Julien, J.L., Gousset-
968 Dupont, A., Fumanal, B., Label, P., Pujade-Renaud, V., Auguin, D., Venisse J.S., 2016. The
969 *Hevea brasiliensis* XIP aquaporin subfamily: genomic, structural and functional
970 characterizations with relevance to intensive latex harvesting. Plant Molecular Biology 91,
971 375-396.

972 Martin, C.E., Lin, T.C., Lin, K.C., Hsu, C.C., Chiou, W.L., 2004. Causes and consequences of
973 high osmotic potentials in epiphytic higher plants. Journal of Plant Physiology 161, 1119-
974 1124.

975 Martin-StPaul, N., Delzon, S., Cochard, H., 2017. Plant resistance to drought depends on
976 timely stomatal closure. Ecology Letters, doi: 10.1111/ele.12851.

977 Mertz, R.A., Brutnell, T.P., 2014. Bundle sheath suberization in grass leaves: multiple
978 barriers to characterization. Journal of Experimental Botany 65, 3371-3380.

979 Maurel, C., Tacnet, F., Guclu, J., Guern, J., Ripoche, P., 1997. Purified vesicles of tobacco
980 cell vacuolar and plasma membrane exhibit dramatically different water permeability and
981 water channel activity. PNAS 94, 7103-7108.

982 Nobel, P.S., 2006. Parenchyma-chlorenchyma water movement during drought for the
983 hemiepiphytic cactus Hylocereus undatus. Annals of Botany 97, 469-474.

984 Ohtsuka, A., Sack, L., Taneda, H., 2017. Bundle sheath lignification mediates the linkage of
985 leaf hydraulics and venation. Plant Cell Environ. 18, 1-12.

986 Pfaffl, M.W., Tichopad, A., Prgomet, C., Neuvians, T.P., 2004. Determination of stable
987 housekeeping genes, differentially regu- lated target genes and sample integrity:
988 BestKeeper–Excel-based tool using pair-wise correlations. Biotechnology Letter 26, 509-515.

989 Pou, A., Medrano, H., Flexas, J., Tyerman, S.D., 2013. A putative role for TIP and PIP
990 aquaporins in dynamics of leaf hydraulic and stomatal conductances in grapevine under
991 water stress and re-watering. Plant Cell Environment 36, 828-843.

992 Prado, K., Maurel, C., 2013. Regulation of leaf hydraulics: from molecular to whole plant
993 levels. Frontiers in Plant Science 4, 58-60.

Prado, K., Boursiac, Y., Tournaire-Roux, C., Monneuse, J.M., Postaire, O., Da Ines, O., Maurel, C., 2013. Regulation of *Arabidopsis* leaf hydraulics involves light-dependent phosphorylation of aquaporins in veins. Plant Cell 25, 1029-1039.

R Core Team (2017). R: A language and environment for statistical computing. R Foundation for Statistical Computing, Vienna, Austria. URL https://www.R-project.org/.

Rockwell, F.E., Holbrook, N.M., 2017. Leaf Hydraulic Architecture and Stomatal Conductance: A Functional Perspective. Plant Physiology 174, 1996-2007.

Sack, L., Melcher, P.J., Zwieniecki, M.A., Holbrook, N.M., 2002. The hydraulic conductance of the angiosperm leaf lamina: a comparison of three measurement methods. Journal of Experimental Botany 53, 2177-2184.

Sack, L., Holbrook, N.M., 2006. Leaf hydraulics. Annu. Rev. Plant Biol. 57, 361-381.

Sack, L., Cowan, P.D., Jaikumar, N., Holbrook, N.M., 2003. The 'hydrology' of leaves: co-ordination of structure and function in temperate woody species. Plant Cell and Environment 26, 1343-1356.

Sack, L., Pasquet-Kok, J., 2011. http://www.publish.csiro.au/prometheuswiki/tiki-pagehistory.php?page=Leaf pressure-volume curve parameters&preview=16.

Sack, L., Scoffoni, C., 2013. Leaf venation: structure, function, development, evolution, ecology and applications in the past, present and future. New Phytologist 198, 983-1000.

Sade, N., Shatil-Cohen, A., Attia, Z., Maurel, C., Boursiac, Y., Kelly, G., Granot, D., Yaaran, A., Lerner, S., Moshelion, M., 2014. The role of plasma membrane aquaporins in regulating the bundle sheath-mesophyll continuum and leaf hydraulics. Plant Physiology 166, 1609-1620.

Sade, N., Moshelion, M. 2016. Plant aquaporins and abiotic stress. In Plant Aquaporins: From Transport to Signalling; Chaumont, F., Tyerman, S., Eds.; Spinger-Verlag: Berlin-Heidelberg, Germany.

Sakr, S., Alves, G., Morillon, R., Maurel, K., Decourteix, M., Guillot, A., Fleurat-Lessard, P., Julien, J.L., Chrispeels, M.J., 2003. Plasma membrane aquaporins are involved in winter embolism recovery in walnut tree. Plant Physiology 133, 630-641.

Schmidt, J.E., Kaiser, W.M., 1987. Response of the succulent leaves of *Peperomia magnoliaefolia* to dehydration. Plant Physiology 83, 190-194.

Scholz, F.G., Bucci, S.J., Hoffmann, W.A., Meinzer, F.C., Goldstein, G., 2010. Hydraulic lift in a neotropical savanna: experimental manipulation and model simulations. Agric For Meteorol 150, 629–639

1027 Scoffoni, C., Jansen, S., 2016. I Can See Clearly Now - Embolism in Leaves. Trends in Plant
1028 Science 21, 723-725.

1029 Scoffoni, C., Albuquerque, C., Brodersen, C.R., Townes, S.V., John, G.P., Cochard, H.,
1030 Buckley, T.N., McElrone, A.J., Sack, L., 2017a. Leaf vein xylem conduit diameter influences
1031 susceptibility to embolism and hydraulic decline. New Phytologist 213, 1076-1092.

1032 Scoffoni, C., Albuquerque, C., Brodersen, C.R., Townes, S.V., Grace, P.J., Bartlett, M.K.
1033 Buckley, T.N., McElrone, A.J., Sack, L., 2017b. Outside-Xylem Vulnerability, Not Xylem
1034 Embolism, Controls Leaf Hydraulic Decline during Dehydration. Plant Physiol, 173,1997-
1035 1210.

1036 Secchi, F., Maciver, B., Zeidel, M.L., Zwieniecki, M.A., 2009. Functional analysis of putative
1037 genes encoding the PIP2 water channel subfamily Populus trichocarpa. Tree Physiology 29,
1038 1467-1477.

1039 Secchi, F., Zwienecki, M.A., 2010. Patterns of PIP gene expression in *Populus trichocarpa*
1040 during recovery from xylem embolism suggest a major role for the PIP1 aquaporin subfamily
1041 as moderators of refilling process. Plant Cell Environ 33, 1285-1297.

1042 Shatil-Cohen, A., Attia, Z. Moshelion, M., 2011. Bundle-sheath cell regulation of xylem-
1043 mesophyll water transport via aquaporins under drought stress: a target of xylem-borne
1044 ABA? Plant J 67, 72-80.

1045 Smith, J.A.C., Schulte, P.J., Nobel, P.S., 1987. Water flow and water storage in *Agave*
1046 *deserti*: osmotic implications of Crassulacean acid metabolism. Plant Cell and Environment
1047 10, 639-648.

1048 Sommerville, K.E., Sack, L., Ball, M.C., 2012. Hydraulic conductance of Acacia phyllodes
1049 (foliage) is driven by primary nerve (vein) conductance and density. Plant, Cell and
1050 Environment 35, 158-168.

1051 Steppe, K., De Pauw, D.J.W., Lemeur, R., Vanrolleghem, P.A. 2006. A mathematical model
1052 linking tree sap flow dynamics to daily stem diameter fluctuations and radial stem growth.
1053 Tree Physiology 26, 257-273.

1054 Terashima, I., 1992. Anatomy of non-uniform leaf photosynthesis. Photosynth Res. 31, 195-
1055 212.

1056 Tissue, D.T., Yakir, D., Nobel, P.S., 1991. Diel water movement between parenchyma and
1057 chlorenchyma of two desert CAM plants under dry and wet conditions. Plant Cell and
1058 Environment 14, 407-413.

1059 Tyree, M.T., Hammel, H.T. 1972. The measurement of the turgor pressure and the water
1060 relations of plants by the pressure-bomb technique. J. Exp. Bot. 23, 267-282.

1061 Tyree, M.T., Alexander, J., Machado, J.L., 1992. Loss of hydraulic conductivity due to water
1062 stress in intact juveniles of *Quercus rubra* and *Populus deltoides*. Tree Physiology 10, 411-
1063 415.

1064 van den Honert, T.H., 1948. Water transport in plants as a catenary process. Discuss
1065 Faraday Soc 3, 146-153.

1066 Vendramini, F., Diaz, S., Gurvich, D.E., Wilson, P.J., Thompson, K., Hodgson, J.G., 2002.
1067 Leaf traits as indicators of resource-use strategy in floras with succulent species. New
1068 Phytologist 154, 147-157.

1069 Vitali, M., Cochard, H., Gambino, G., Ponomarenko, A., Perrone, I., Lovisolo, C., 2016.
1070 VvPIP2;4N aquaporin involvement in controlling leaf hydraulic capacitance and resistance in
1071 grapevine. Physiologia Plantarum. 158, 284-296.

1072 Warnes, G.R., Ben Bolker, W., Bonebakker, L., Gentleman, R., Liaw, W.H.A., Lumley, T.,
1073 Maechler, M., Magnusson, A., Moeller, S., Schwartz, M., Venables, B., 2016. gplots: Various
1074 R Programming Tools for Plotting Data. R package version 3.0.1.

1075 Wheeler, J.K., Huggett, B.A., Tofte, A.N., Rockwell, F.E., Holbrook, N.M., 2013. Cutting
1076 xylem under tension or supersaturated with gas can generate PLC and the appearance of
1077 rapid recovery from embolism. Plant, Cell and Environment 36, 1938-1949.

1078 Williams M.L., Thomas B.J., Farrar J.F., Pollock C.J., 1993. Visualizing the distribution of
1079 elements within Barley leaves by energy-dispersive x-ray image maps (Edx Maps). New
1080 Phytologist 125, 367-372.

1081 Xu, M., Zhang, B., Su, X., Zhang, S., Huang, M., 2011. Reference gene selection for
1082 quantitative real-time polymerase chain reaction in Populus. Anal. Biochem. 408, 337-339.

1083 Zelazny, E., Borst, J.W., Muylaert, M., Batoko, H., Hemminga, M.A., Chaumont, F., 2007.
1084 FRET imaging in living maize cells reveals that plasma membrane aquaporins interact to
1085 regulate their subcellular localization. Proc Natl Acad Sci USA 104, 12359-12364.